available at www.sciencedirect.com
journal homepage: www.europeanurology.com

European Association of Urology

Platinum Priority – Prostate Cancer

Editorial by Shilpa Gupta and Hannelore V. Heemers on pp. 734–735 of this issue

Taxane-induced Attenuation of the CXCR2/BCL-2 Axis Sensitizes Prostate Cancer to Platinum-based Treatment

Vicenç Ruiz de Porras [a,b], Xieng C. Wang [c,†], Luis Palomero [c,†], Mercedes Marin-Aguilera [d], Carme Solé-Blanch [a,b], Alberto Indacochea [e,f], Natalia Jimenez [d], Sara Bystrup [a,g], Martin Bakht [h], Vincenza Conteduca [h,i], Josep M. Piulats [c,j], Oscar Buisan [k], José F. Suarez [c,l], Juan Carlos Pardo [b,m], Elena Castro [n,o], David Olmos [n,o], Himisha Beltran [h], Begoña Mellado [d,p], Eva Martinez-Balibrea [a,g], Albert Font [b,m,], Alvaro Aytes [c,g,*]*

[a] *Germans Trias i Pujol Research Institute (IGTP), Badalona, Spain;* [b] *Catalan Institute of Oncology, Badalona Applied Research Group in Oncology (BARGO), Badalona, Spain;* [c] *Program of Molecular Mechanisms and Experimental Therapeutics in Oncology, Bellvitge Institute for Biomedical Research (IDIBELL), L'Hospitalet de Llobregat, Gran Via de L'Hospitalet, Barcelona, Spain;* [d] *Translational Genomics and Targeted Therapeutics in Solid Tumors Laboratory, Institut d'Investigacions Biomèdiques August Pi i Sunyer (IDIBAPS), Barcelona, Spain;* [e] *Centre for Genomic Regulation (CRG), The Barcelona Institute of Science and Technology, Barcelona, Spain;* [f] *Universitat Pompeu Fabra (UPF), Barcelona, Spain;* [g] *Program Against Cancer Therapeutics Resistance (ProCURE), Catalan Institute of Oncology, Gran Via de L'Hospitalet, Barcelona, Spain;* [h] *Department of Medical Oncology, Dana Farber Cancer Institute, Boston, MA, USA;* [i] *Instituto Scientifico Romagnolo per lo Studio e la Cura dei Tumori (IRST), IRCCS, Meldola, Italy;* [j] *Department of Medical Oncology, Catalan Institute of Oncology (ICO), Hospitalet de Llobregat, Barcelona, Spain;* [k] *Department of Urology, Hospital Germans Trias I Pujol, Badalona, Spain;* [l] *Department of Urology, Bellvitge University Hospital, Hospitalet de Llobregat, Barcelona, Spain;* [m] *Department of Medical Oncology, Catalan Institute of Oncology, Badalona, Spain;* [n] *Genitourinary Cancer Translational Research Group, The Institute of Biomedical Research in Málaga, Málaga, Spain;* [o] *Prostate Cancer Clinical Research Unit, Spanish National Cancer Research Centre, Madrid, Spain;* [p] *Department of Medical Oncology, Hospital Clínic, Barcelona, Spain*

Article info

Article history:
Accepted October 2, 2020

Associate Editor:
T Morgan

Keywords:
Combination treatment
Metastatic castration-resistant prostate cancer
Taxane resistance
Platinum

Abstract

Background: Taxanes are the most active chemotherapy agents in metastatic castration-resistant prostate cancer (mCRPC) patients; yet, resistance occurs almost invariably, representing an important clinical challenge. Taxane-platinum combinations have shown clinical benefit in a subset of patients, but the mechanistic basis and biomarkers remain elusive.
Objective: To identify mechanisms and response indicators for the antitumor efficacy of taxane-platinum combinations in mCRPC.
Design, setting, and participants: Transcriptomic data from a publicly available mCRPC dataset of taxane-exposed and taxane-naïve patients were analyzed to identify response indicators and emerging vulnerabilities. Functional and preclinical validation was performed in taxane-resistant mCRPC cell lines and genetically engineered mouse models (GEMMs).
Intervention: Metastatic CRPC cells were treated with docetaxel, cisplatin, carboplatin, the CXCR2 antagonist SB265610, and the BCL-2 inhibitor venetoclax. Gain and loss of function in culture of CXCR2 and BCL-2 were achieved by overexpression or siRNA silencing. Preclinical assays in GEMM mice tested the antitumor efficacy of taxane-platinum combinations.

† These authors contributed equally.
* Corresponding authors. Catalan Institute of Oncology, Badalona, Spain (A. Font); Bellvitge Institute for Biomedical Research, Gran Via de LHospitalet, Barcelona, Spain. Tel. +34 932607464 (A. Aytes).
E-mail addresses: afont@iconcologia.net (A. Font), aaytes@idibell.cat (A. Aytes).

https://doi.org/10.1016/j.eururo.2020.10.001

Outcome measurements and statistical analysis: Proliferation, apoptosis, and colony assays measured drug activity in vitro. Preclinical endpoints in mice included growth, survival, and histopathology. Changes in CXCR2, BCL-2, and chemokines were analyzed by reverse transcriptase quantitative polymerase chain reaction and Western blot. Human expression data were analyzed using Gene Set Enrichment Analysis, hierarchical clustering, and correlation studies. GraphPad Prism software and R-studio were used for statistical and data analyses.
Results and limitations: Transcriptomic data from taxane-exposed human mCRPC tumors correlate with a marked negative enrichment of apoptosis and inflammatory response pathways accompanied by a marked downregulation of CXCR2 and BCL-2. Mechanistically, we show that docetaxel inhibits CXCR2 and that BCL-2 downregulation occurs as a downstream effect. Further, we demonstrated in experimental models that the sensitivity to cisplatin is dependent on CXCR2 and BCL-2, and that targeting them sensitizes prostate cancer (PC) cells to cisplatin. In vivo taxane-platinum combinations are highly synergistic, and previous exposure to taxanes sensitizes mCRPC tumors to second-line cisplatin treatment.
Conclusions: The hitherto unappreciated attenuation of the CXCR2/BCL-2 axis in taxane-treated mCRPC patients is an acquired vulnerability with potential predictive activity for platinum-based treatments.
Patient summary: A subset of patients with aggressive and therapy-resistant prostate cancer benefits from taxane-platinum combination chemotherapy; however, we lack the mechanistic understanding of how that synergistic effect occurs. Here, using patient data and preclinical models, we found that taxanes reduce cancer cell escape mechanisms to chemotherapy-induced cell death, hence making these cells more vulnerable to additional platinum treatment.

1. Introduction

Despite significant initial responses to androgen deprivation therapy, most metastatic patients progress to an incurable castration-resistant prostate cancer (mCRPC) [1,2]. Many drugs have been approved for the treatment of mCRPC, including taxanes, and androgen receptor (AR) signaling inhibitors [2,3]. Sadly, in patients progressing to these agents, very few therapeutic options are available, although platinum-based treatments have demonstrated a limited benefit in patients with aggressive variant prostate cancer (PC) [4–6]. Predictive markers are needed to determine the best treatment for patients previously treated with taxanes or AR signaling inhibitors.

Taxanes bind tubulin-inhibiting mitosis but also AR nuclear translocation, reducing AR signaling [7–9]. Several factors are associated with taxane resistance, including expression of β-tubulin isoforms and activation of drug efflux pumps. PTEN loss and activation of PI3K/AKT/mTOR, MAPK, and NF-kB have also been associated with taxane resistance [10,11]. While platinum agents are not used routinely for the treatment of mCRPC, there is an increasing use of these agents, especially in patients with small-cell or neuroendocrine tumor variants [6]. In fact, some antitumor activity has been described for carboplatin, cisplatin, and satraplatin in mCRPC patients [12]. Unfortunately, molecular biomarkers to identify mCRPC patients who could benefit from these drug combinations remain elusive. The incomplete understanding of the molecular mechanisms of taxane resistance limits the identification of vulnerabilities and potential therapeutic targets.

Here, we sought to elucidate the mechanistic basis and response indicators for the synergistic antitumor efficacy of taxane-platinum combinations in advanced PC (Supplementary Fig. 1). Mining of human PC datasets to compare the transcriptomes of taxane-exposed and taxane-naïve patients showed a marked downregulation of CXCR2 and BCL-2 in taxane-exposed patients. Mechanistically, we showed that taxanes induce CXCR2 and BCL-2 downregulation. Further, we demonstrated that CXCR2 and BCL-2 determine cisplatin sensitivity and that targeting them sensitizes PC cells to cisplatin. Finally, in vivo preclinical data testing show that taxane-platinum combinations are highly synergistic and that previous exposure to taxanes sensitizes mCRPC tumors to cisplatin. Together, our data identify an acquired vulnerability in taxane-treated mCRPC patients with a potential predictive value for platinum-based drug combinations.

2. Materials and methods

See the Supplementary material for further detail.

2.1. Computational analysis of human PC data

Human transcriptome data [13,14] were used for gene expression (Supplementary Table 1) and pathway enrichment using Gene Set Enrichment Analysis (GSEA; Supplementary Table 2). Univariate analyses were performed using Spearman rank correlation tests. For bivariate analysis, linear regressions were performed (Supplementary Table 3). False discovery rate and bootstrapping were performed when appropriate, to correct for multiple testing.

2.2. Functional assays in vitro

Docetaxel-resistant DU145-DR and PC3-DR human PC cells had been generated previously [15]. Docetaxel, cabazitaxel, cisplatin, carboplatin (MedChemExpress; Monmouth Junction, NJ, USA), CXCR2 antagonist

SB265610 (Sigma Aldrich; St. Louis, MO, USA), and BCL-2 inhibitor venetoclax (MedChemExpress; Monmouth Junction, NJ, USA) were prepared in dimethyl sulfoxide. Western blot, cell viability, apoptosis, and gain and loss of function studies were performed as described previously [16]. Oligonucleotides and antibodies are listed in Supplementary Table 4.

2.3. Preclinical assays in vivo

Animal studies were approved by the Institutional Review Board at IDIBELL. The NPK mouse model had been published previously [17]. For tumor growth and survival assays, allografted NPK tumor-bearing mice were enrolled in preclinical studies.

2.4. Immunohistochemical analysis

Immunostaining of mouse prostate tumor tissues was performed, as described previously [18], on formalin-fixed paraffin-embedded sections incubated with primary and secondary antibodies shown in Supplementary Table 4.

2.5. Statistical analysis

Statistical differences were calculated using nonlineal regression and F test for viability, or two-tailed Student t test for clonogenicity and apoptosis; $p < 0.05$ was considered significant. One-way analysis of variance was used for vehicle and each treatment group in in vivo preclinical assays. In survival analysis, p values were calculated using a log-rank test. Radiographic progression was defined using Response Evaluation Criteria in Solid Tumors version 1.1. A decline in prostate-specific antigen (PSA) was evaluated according to Prostate Cancer Clinical Trials Working Group 3 (PCWG3) guidelines (PSA decline $\geq$ 50%) to the date of radiographic progression of disease. Radiographic progression-free survival was estimated by the Kaplan-Meier method and compared using the log-rank or Fisher exact test. PSA decline was evaluated using Fisher exact test, with a significance level of 5% used to measure the association with PSA decline.

3. Results

3.1. The CXCR2/BCL-2 axis is attenuated in human PC exposed to taxane

We investigated the transcriptomic changes in mCRPC tumors exposed to taxanes in a human PC dataset [13]. GSEA identified significantly enriched hallmark cancer pathways (Supplementary Fig. 2A and Supplementary Table 2) including "androgen response" (normalized enrichment score [NES] = −2.002; false discovery rate [FDR] q value = 8.16×10^{-5}). Interestingly, "apoptosis" (NES = –1.817; FDR q value = 5.76×10^{-4}) and "inflammatory response" (NES = –1.933964; FDR q value = 2.05×10^{-4}) pathways were enriched negatively in taxane-exposed mCRPC tumors (Fig. 1A and B), prompting us to hypothesize a role in platinum treatment response, as we showed previously in other tumor types [16]. A comparison of gene expression changes between the significantly enriched pathways showed only the "interferon alpha and gamma" pathways as marginally differentially expressed compared with "apoptosis" and "inflammatory response" ($p = 0.017$ and $p = 0.038$, respectively; Fig. 1C). Moreover, the mean expression was significantly lower than that of a random model equally sized to the top differentially expressed genes ($p < 0.001$) between taxane-naïve and taxane-exposed tumors, and similar to that of a multigene signature using all genes in the leading edge of the significantly enriched pathways (Supplementary Fig. 2B).

Unsupervised clustering of the GSEA leading-edge genes from the "apoptosis" significantly segregated patients exposed to taxanes in the SU2C dataset ($p = 0.004$; Fig. 1D). Significantly downregulated genes included the antiapoptotic master regulator *BCL-2* ($p = 0.007$), as well as *CXCL8* ($p = 0.043$) and *CXCL6* ($p = 0.007$; Supplementary Table 1), known to bind the CXCR2 receptor and trigger antiapoptosis programs [19]. In fact, *CXCR2* and *BCL-2* expression levels are significantly correlated with the negative enrichment of the "apoptosis" pathway in taxane-exposed patients but not in taxane-naïve ones ($p = 0.04$ and $p = 0.030$, respectively; Fig. 1E and Supplementary Table 3), and are associated with decreased AR and increased neuroendocrine PC scores (Supplementary Fig. 2C and D). Moreover, *CXCR2* and *BCL-2* mRNA levels were found significantly downregulated ($p = 0.042$ and $p = 0.001$, respectively) in an independent human dataset (Fig. 1F) [14]. Together, these data indicate that taxane treatment attenuates the antiapoptotic signaling mediated by CXCR2 and BCL-2 in mCRPC patients.

3.2. Docetaxel induces CXCR2/BCL-2 downregulation in vitro and in vivo

We next asked whether CXCR2/BCL-2 downregulation was causally linked to taxane exposure. We observed an immediate downregulation of CXCR2 and BCL-2 in docetaxel-treated DU145 and PC3 cells (Fig. 2A). In agreement with the in vitro observation, tumors from the docetaxel-treated NPK mice showed a marked reduction in CXCR2 and BCL-2 compared with nontreated controls (Fig. 2B). Importantly, this downregulation of CXCR2 and BCL-2 upon taxane exposure was also observed in p53-proficient LNCaP cells (Supplementary Fig. 3I).

Next, we evaluated CXCR2 and BCL-2 levels in docetaxel-resistant cell derivatives, namely, DU145-DR and PC3-DR (Supplementary Fig. 3A). Consistently, protein levels of CXCR2 and BCL-2 in untreated DU145-DR and PC3-DR cells were reduced profoundly (Fig. 2C). In addition, CXCR2 ligands *CXCL8* and *CXCL6* were also significantly downregulated (Supplementary Fig. 3B), as was *CXCR1*, which is coregulated with CXCR2 (Supplementary Fig. 3C) [20]. Notably, reduced *CXCR2* expression was not due to promoter hypermethylation, as treatment with the 5-AZA did not increase protein expression (Supplementary Fig. 3C and D).

Depletion of CXCR2 or CXCL8/CXCL6 has been shown to promote BCL-2 downregulation in different tumor types [16,21,22]. In fact, silencing of CXCR2 in parental DU145 and PC3 cells (Supplementary Fig. 3E) induced a marked reduction in BCL-2 protein expression compared with control cells (Fig. 2D). Additionally, DU145-DR cells, which are depleted of CXCR2, were four-fold more resistant to CXCR2 inhibitor SB265610 than parental cells ($p < 0.0001$; Fig. 2E). Conversely, CXCR2 overexpression significantly

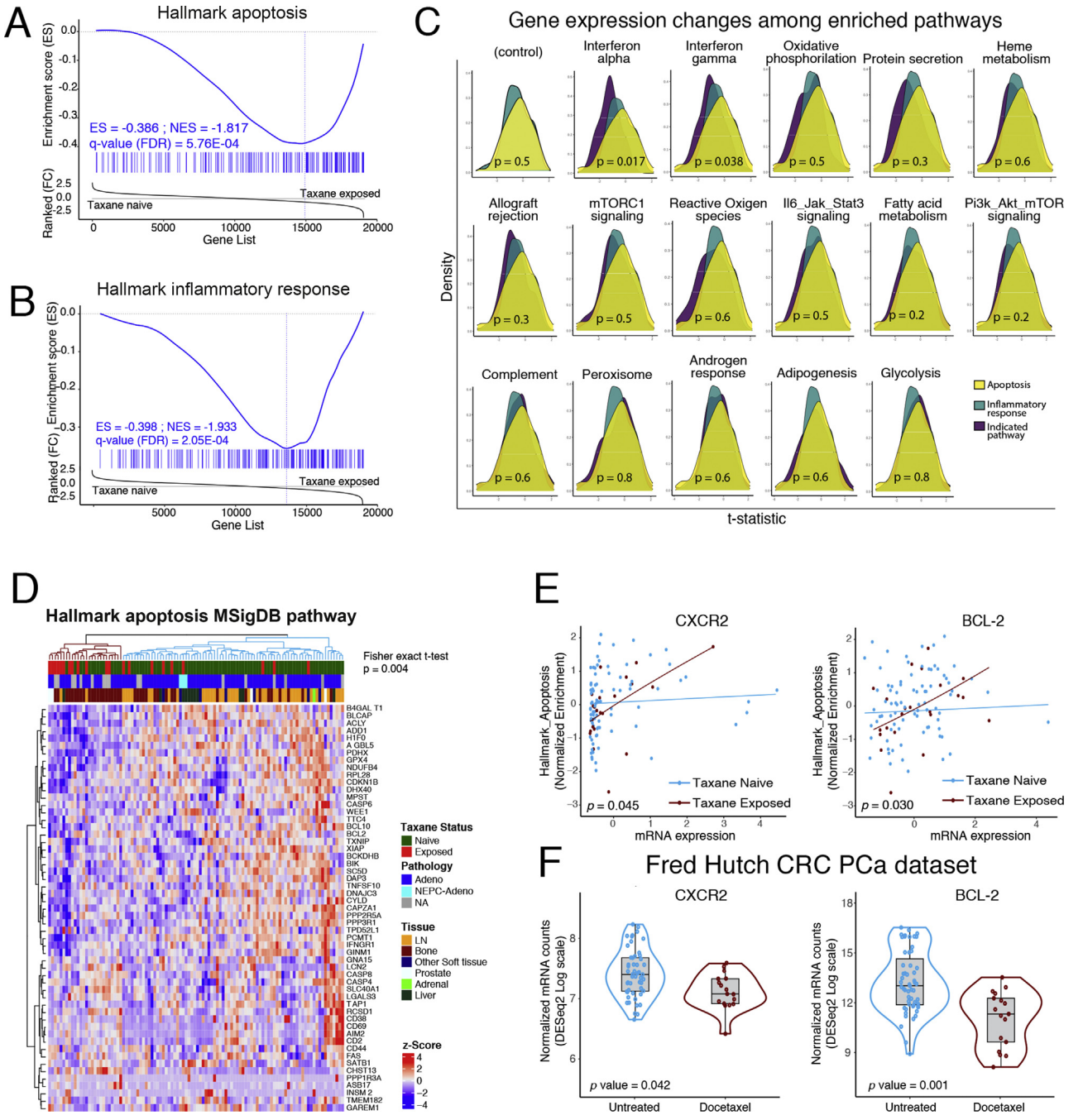

Fig. 1 – CXCR2 and BCL-2 are downregulated in human prostate cancer exposed to taxane. GSEA showing a significant negative enrichment for the (A) apoptosis and (B) inflammatory response pathways from the hallmarks pathways of the MSigDB in the differential gene expression signature of the taxane-naïve versus taxane-exposed tumors in the SU2C dataset. (C) Density plots show the difference in the median gene expression change between the apoptosis and inflammatory response pathways (control) and between these two pathways and each of the top significantly enriched (by GSEA) pathways using nonparametric Kruskal-Wallis test. (D) Unsupervised clustering of patients according to the gene expression of the leading-edge genes from the GSEA in (B). The Fisher exact *t* test *p* value for the association of taxane-exposed status and downregulation of the signature are shown in the heatmap. (E) Linear regressions for the correlation between *CXCR2* (left) and *BCL-2* (right) expression and the normalized enrichment score of the apoptosis pathway. Taxane-exposed and taxane-naïve patients are shown separately. The *p* value indicates the significance of the differential association between gene expression and pathway enrichment using *t* test. (F) Differences in mRNA expression between taxane-exposed and taxane-naïve patients in the FHCRC dataset for *CXCR2* (left) and *BCL-2* (right) using *t* test. Control for multiple testing was performed using false discovery rate adjustment on differential expression, pathway enrichment, and bootstrapping for correlation analysis. ES = enrichment score; FC = fold change; FDR = false discovery rate; GSEA = Gene Set Enrichment Analysis; LN = lymph node; NA = not available; NES = normalized enrichment score.

sensitized PC3-DR cells to docetaxel ($p = 0.019$; Fig. 2F and G, and Supplementary Fig. 3F). Similarly, BCL-2 overexpression in DU145-DR and PC3-DR cells (Supplementary Fig. 3G) resulted in a significant change in docetaxel sensitivity ($p = 0.012$ and $p < 0.0001$, respectively; Fig. 2H and I), apoptosis ($p = 0.040$ and $p = 0.021$, respectively; Fig. 2J and K), and clonogenicity ($p = 0.021$ in PC3-DR cells; Fig. 2L and M).

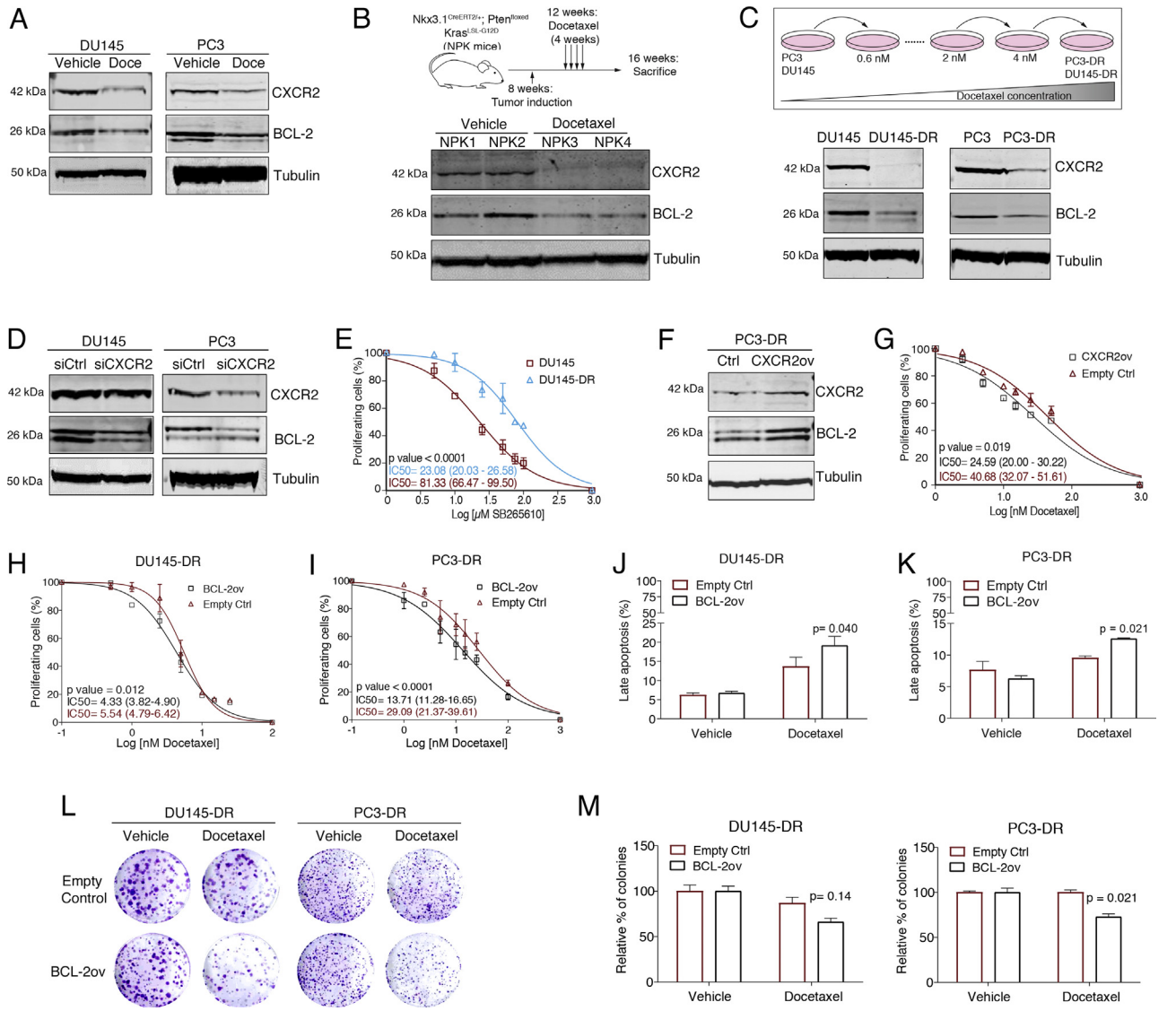

Fig. 2 – Effect of docetaxel treatment on CXCR2/BCL-2 axis regulation. (A) Representative Western blot images (*n* = 3) showing protein expression changes of CXCR2 and BCL-2 in DU145 and PC-3 cells after treatment with docetaxel (Doce) at 6.5 and 15 nM, respectively, for 72 h; α-tubulin was used as an endogenous control. (B) Experimental strategy: 1 mo after tamoxifen-mediated induction of the cre-dependent, recombination, tumor-bearing mice (*n* = 4) were exposed to four cycles of docetaxel treatment (oral gavage, 2 mg/kg, Monday to Friday) or vehicle (top). Western blot showing CXCR2 and BCL-2 protein expression changes in tumor tissues from NPK GEMM exposed to docetaxel or vehicle; α-tubulin was used as an endogenous control (bottom). (C) Experimental strategy: DU145 and PC3 cells were converted to docetaxel-resistant cells by exposing them to increasing doses of docetaxel in an intermittent regimen during 1 yr and 6 mo, respectively (top). Western blot analysis (*n* = 3) of CXCR2 and BCL-2 basal protein expression in PC3/PC3-DR and DU145/DU145-DR cell lines; α-tubulin was used as an endogenous control (bottom). (D) Representative western blot images (*n* = 3) showing changes in CXCR2 and BCL-2 protein expression in PC3 and DU145 cells under negative control (siCtrl) and *CXCR2* (siCXCR2) gene silencing; α-tubulin was used as an endogenous control. (E) Dose-response curves for DU145 and DU145-DR cells after SB265610 treatment at 0–100 μM for 72 h (mean ± SEM). (F) Western blot analysis (*n* = 3) of CXCR2 and BCL-2 protein expression changes under empty control (Crtl) and *CXCR2* overexpression (CXCR2ov) in PC3-DR cells; α-tubulin was used as and endogenous control. (G) Dose-response curves for PC3-DR cell line, after CXCR2ov, treated with 0–50 nM docetaxel for 72 h (mean ± SEM). Dose-response curves for (H) DU145-DR and (I) PC3-DR cell lines, after *BCL-2* overexpression (BCL-2ov), treated with 0–50 nM docetaxel for 72 h. Bar graph representing the percentage (mean ± SEM) of late apoptotic cells after 72 h of treatment with docetaxel in (J) DU145-DR (5 nM) and (K) PC3-DR (15 nM) after BCL-2ov. The *p* value was relative to cells transfected with an empty vector (Empty Ctrl) treated with docetaxel. (L) Representative colony assay images after treatment with docetaxel at 0.5 nM for 72 h in DU145-DR and PC3-DR cells, after BCL-2ov. (M) Bar graph representing the percentage (mean ± SEM) of colonies after 72 h of treatment with docetaxel in DU145-DR (left) and PC3-DR (right) after BCL-2ov. The *p* value was relative to cells transfected with an empty vector (Empty Ctrl) treated with docetaxel. Results were obtained from at least three independent biological replicates. The *p* values were calculated using nonlineal regression and *F* test for viability, or two-tailed Student *t* test for clonogenicity and apoptosis, and considered significant when <0.05. IC50 = half maximal inhibitory concentration; SEM = standard error of the mean.

Collectively, these results demonstrate that docetaxel induces a downregulation of CXCR2 and BCL-2, in vitro and in vivo, and that this downregulation is maintained after docetaxel resistance is established.

3.3. *Downregulation of CXCR2/BCL-2 sensitizes PC cells to platinum*

Inhibition of CXCR2 signaling and its downstream effector BCL-2 increases the sensitivity of tumor cells to platinum

drugs [16,22,23]. Based on our results indicating that docetaxel triggers a marked reduction in the CXCR2/BCL-2 axis, and the clinical benefit observed for the combination of platinum and taxanes in mCRPC [24], we hypothesized that the sensitivity of docetaxel-resistant PC cells to platinum treatment might be CXCR2/BCL-2 dependent. As predicted, docetaxel-resistant DU145-DR and PC3-DR cells were significantly more sensitive to cisplatin and carboplatin than their respective parental cells (DU145-DR, $p = 0.004$ and $p < 0.0001$; PC3-DR $p < 0.0001$ and $p < 0.0001$ for cisplatin and carboplatin, respectively; Fig. 3A and B). In agreement with the observed downregulation of antiapoptotic signaling in the taxane-treated patients of the SU2C human PC cohort, cisplatin induced a significant dose-dependent increase in late apoptosis rates in the docetaxel-resistant DU145-DR cells, as compared with parental DU145 cell line ($p = 0.041$ and $p = 0.019$ for 2.5 and 5 μM of cisplatin, respectively; Fig. 3C and D, and Supplementary Fig. 3K and L), which was also confirmed in clonogenic assays (Fig. 3E–G).

To ascertain the role of CXCR2 and BCL-2 in cisplatin sensitivity, we silenced them and assessed the cytotoxicity of cisplatin. Silencing of CXCR2 (Fig. 2D and Supplementary Fig. 3E) showed significantly enhanced sensitivity for cisplatin compared with nontargeting siRNA control DU145 and PC3 cells ($p < 0.0001$ and $p < 0.0001$, respectively; Fig. 4A). Similar results were found when BCL-2 was silenced ($p = 0.016$ and $p = 0.0005$, respectively; Fig. 4B and Supplementary Fig. 3H). Importantly, treatment of docetaxel-sensitive DU145 cells with the CXCR2 inhibitor SB265610 significantly sensitized cells to cisplatin in cell viability (Fig. 4C and D) and clonogenic assays (Fig. 4E), which was confirmed in p53-proficient LNCaP cells (Supplementary Fig. 3J). Similarly, treatment of DU145 or PC3 cells with the BCL-2 inhibitor venetoclax enhanced cisplatin sensitivity significantly ($p = 0.023$ and $p < 0.001$, respectively; Fig. 4F and G).

Conversely, overexpression of CXCR2 cells resulted in a significant reduction in cisplatin sensitivity ($p < 0.0001$), an increase in clonogenic capacity ($p = 0.042$), and reduced apoptosis ($p = 0.005$; Fig. 4H and J). This was also observed upon BCL-2 overexpression in either DU145-DR or PC3-DR cells ($p < 0.0001$ and $p < 0.0001$, respectively; Fig. 4K) together with resistance to clonogenic inhibition (-$p = 0.048$ and $p = 0.002$, respectively; Fig. 4L and M) and a dose-dependent reduction in apoptosis (Fig. 4N and O).

Taken together, these data indicate that docetaxel-resistant PC cells are more sensitive to cisplatin treatment and suggest that this vulnerability is in part mediated by the downregulation of the CXCR2/BCL-2 signaling.

3.4. Taxane treatment sensitizes a mouse CRPC model to cisplatin treatment

To test the hypothesis that platinum added to taxane may improve survival and response in aggressive mCRPC, we conducted "preclinical assay 1" in allografted NPK PC models (Fig. 5A). No significant reduction in tumor growth was observed in mice treated with docetaxel, cabazitaxel, or cisplatin alone (Fig. 4B), albeit a modest improvement in survival of mice treated with docetaxel (median survival 65 ± 4.9 vs 55.5 ± 4 d, $p < 0.001$) and cabazitaxel (61 ± 3.14 vs 55.5 ± 4 d, $p = 0.006$), but not with cisplatin (56 ± 1.7 vs 55.5 ± 4 d, $p = 0.3$; Fig. 4D). Comparable results in tumor growth inhibition were found with carboplatin (Supplementary Fig. 4A). Treatments were well tolerated in vivo, and no signs of toxicity were identified at the indicated doses (Supplementary Fig. 4B). Importantly, a significant reduction in tumor growth was observed in docetaxel- or cabazitaxel-cisplatin combinations ($p = 0.0111$ and $p = 0.007$, respectively) and a remarkable improvement in survival (two of 10 reaching endpoint in docetaxel + cisplatin: median survival 75 ± 2.2 vs 55.5 ± 4 d, $p = 1.2 \times 10^{-10}$; none reaching endpoint in cabazitaxel + cisplatin: median survival 75 ± 0 vs 55.5 ± 4 d, $p = 6.8 \times 10^{-12}$; Fig. 5B–D).

We next asked whether previous exposure to taxane sensitizes otherwise resistant tumors to cisplatin treatment. We engrafted mice with control, docetaxel-treated, and cabazitaxel-treated NPK tumors from "preclinical assay 1," and treated them with cisplatin in "preclinical assay 2" (Fig. 5C). Notably, sequential cisplatin after docetaxel or cabazitaxel reduced tumor growth significantly ($p = 0.038$ and $p = 0.029$, respectively) and improved survival (three of 10 reaching endpoint in cisplatin after docetaxel: median survival 40.5 ± 5.5 vs 32.5 ± 2.3 d, $p = 0.00491$; five of 10 reaching endpoint in cisplatin after cabazitaxel: median survival 40.5 ± 4.8 vs 32.5 ± 2.3 d, $p = 0.0019$; Fig. 5E).

We next interrogated a unique retrospective cohort of mCRPC patients who had undergone platinum-based treatment, namely, the Beltran dataset [25]. First, we used the SU2C dataset to stratify patients in high versus low expression of markers. Given the high significant correlation between BCL-2 and CXCR2 expression (Supplementary Fig. 4C) and wide range of gene expression, we used BCL-2 z scores to define the high and low expression groups (z scores < 0.5 as low BCL-2 and z scores > 0.5 as high BCL-2; Supplementary Fig. 4D and E). Interrogation of the Beltran dataset showed a clear trend toward better radiographic progression-free survival in patients with low BCL-2 expression than in patients with high expression (hazard ratio = 3.41, 95% confidence interval 0.74–15.67, $p = 0.09$; Fig. 5F) together with improved PSA responses among the CRPC adenocarcinoma patients ($n = 8$, $p = 0.07$; Fig. 5G). Interestingly, despite this trend not being found using CXCR2 expression alone, the combined use of CXCR2 and BCL-2 showed the best trend ($p = 0.059$; Supplementary Fig. 4F and G).

Analysis of tumor specimens (Fig. 6A and D, and Supplementary Fig. 5A–C) confirmed that the improved antitumor activity of the platinum-based combinations compared with single taxane was associated with a significant reduction of cell proliferation ($p = 0.0027$ and $p = 0.0012$ for docetaxel and cabazitaxel, respectively; Fig. 6B) and antiapoptotic BCL-2 ($p = 0.019$ and $p = 0.010$, respectively) and CXCR2 (Fig. 6C and Supplementary Fig. 5A), together with a marked increase in apoptosis

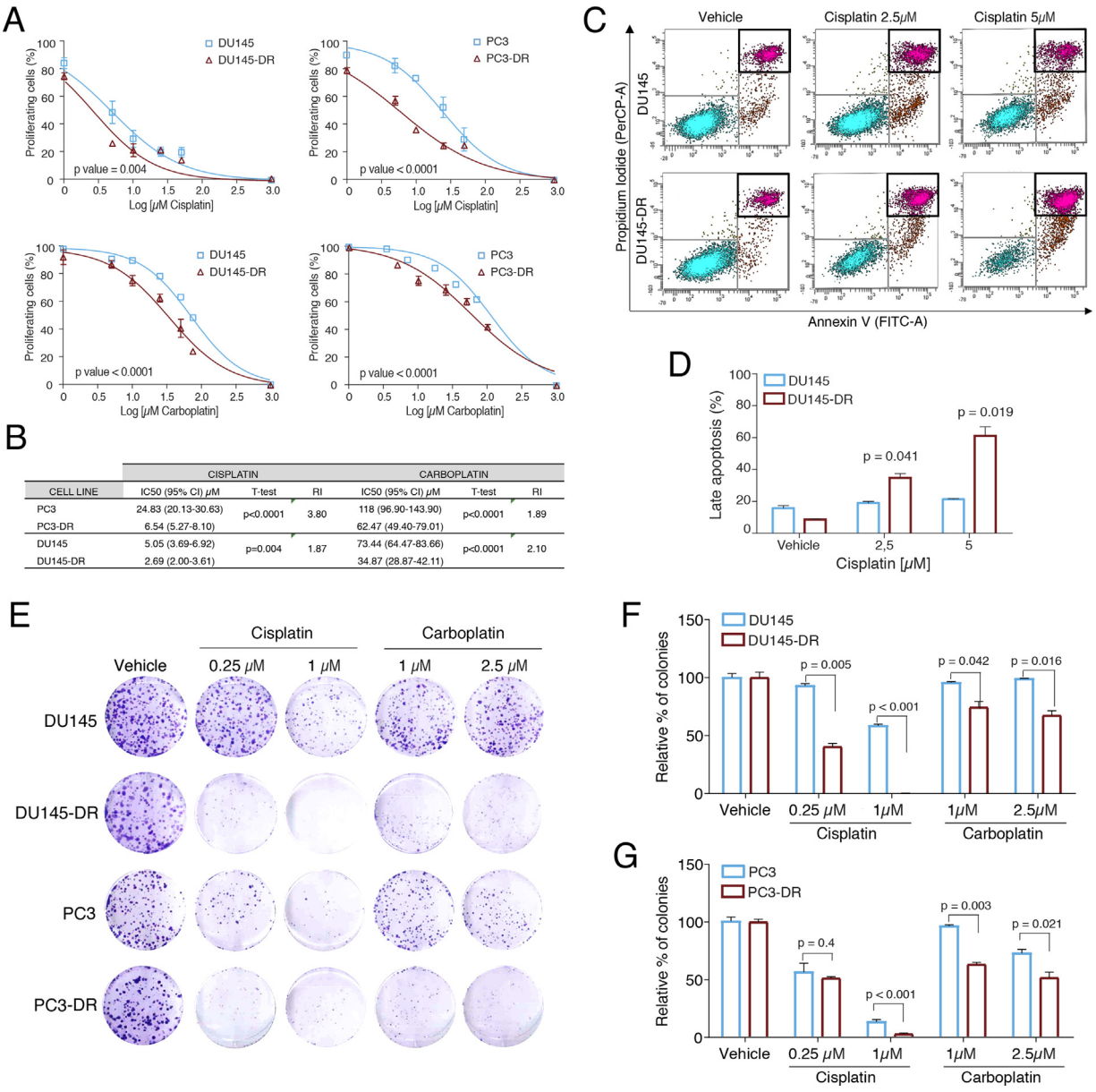

CELL LINE	CISPLATIN IC50 (95% CI) μM	CISPLATIN T-test	CISPLATIN RI	CARBOPLATIN IC50 (95% CI) μM	CARBOPLATIN T-test	CARBOPLATIN RI
PC3	24.83 (20.13-30.63)	p<0.0001	3.80	118 (96.90-143.90)	p<0.0001	1.89
PC3-DR	6.54 (5.27-8.10)			62.47 (49.40-79.01)		
DU145	5.05 (3.69-6.92)	p=0.004	1.87	73.44 (64.47-83.66)	p<0.0001	2.10
DU145-DR	2.69 (2.00-3.61)			34.87 (28.87-42.11)		

Fig. 3 – Docetaxel-resistant cells are more sensitive to platinum treatment. (A) Dose-response curves for DU145/DU145-DR and PC3/PC3-DR cells after cisplatin treatment at 0–50 μM or carboplatin treatment at 0–75 μM for 72 h (mean ± SEM). (B) Table showing cisplatin and carboplatin IC50 values indicated as mean (95% CI) in PC3/PC3-DR and DU145/DU145-DR cell lines. (C) Representative images of apoptosis activation after 72 h of cisplatin treatment of DU145 and DU145-DR cells. (D) Bar graph representing the percentage (mean ± SEM) of late apoptotic cells after 72 h of treatment with cisplatin in DU145 and DU145-DR cell lines at their corresponding IC50 doses—2.5 and 5 μM, respectively; *p* values were relative to parental DU145 cells. (E) Representative colony assay images after treatment with cisplatin or carboplatin at the indicated doses for 24 h in DU145/DU145-DR and PC3/PC3-DR cells. Bar graphs representing the percentage (mean ± SEM) of colonies after 24 h of treatment with cisplatin or carboplatin at the indicated doses in (F) DU145/DU145-DR and (G) PC3/PC3DR cells; *p* values were relative to parental cells treated with cisplatin or carboplatin. Results shown were obtained from at least three independent biological replicates. The *p* values were calculated using nonlineal regression and *F* test for viability, or two-tailed Student *t* test for clonogenic and apoptosis, and considered significant when <0.05. CI = confidence interval; IC50 = half maximal inhibitory concentration; RI = Resistance Index, calculated as the ratio between IC50 of resistant sublines and its corresponding sensitive cell lines; SEM = standard error of the mean.

($p < 0.001$ and $p = 0.004$, respectively; Fig. 6E) and reduced AR ($p < 0.001$ and $p = 0.006$, respectively) in combination treatments (Fig. 6F). Notably, sequential cisplatin after taxane also showed a marked reduction in proliferation and antiapoptotic BCL-2 (Supplementary Fig. 5B).

Taken together, these data strongly suggest that the attenuation of the CXCR2/BCL-2 axis represents a vulnerability in a subset of advanced PC patients and a potential predictive determinant of response to platinum-based chemotherapy that needs to be validated prospectively.

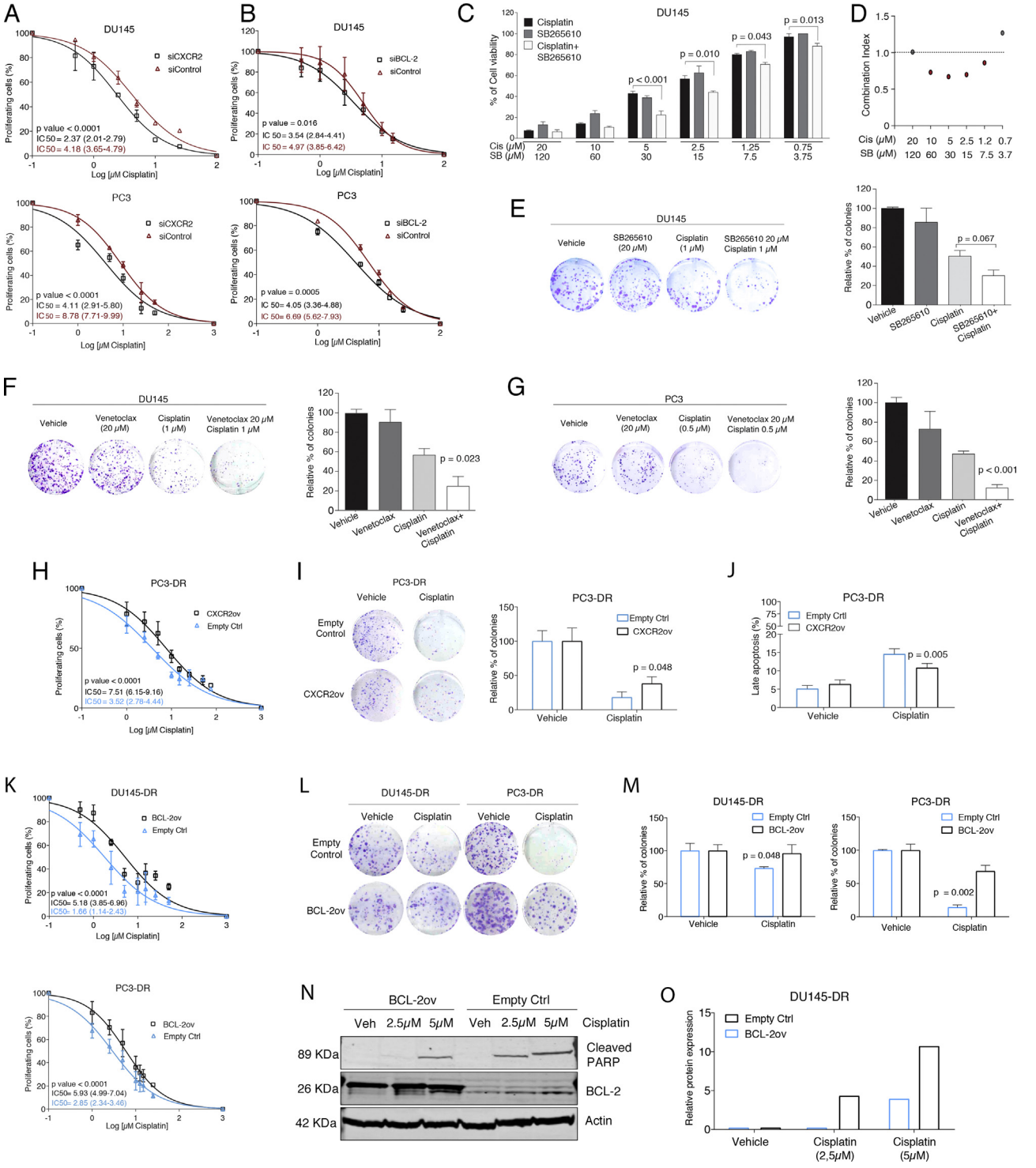

Fig. 4 – Effect of CXCR2 and BCL-2 downregulation and overexpression on platinum sensitivity in PC cells. (A) Dose-response curves for PC3 and DU145 cell lines, after *CXCR2* gene silencing (siCXCR2), treated with 0–50 μM cisplatin for 72 h (mean ± SEM). (B) Dose-response curves for PC3 and DU145 cell lines, after *BCL-2* gene silencing (siBCL-2), treated with 0–50 μM cisplatin for 72 h (mean ± SEM). (C) Bar graphs representing mean ± SEM percentage of cell viability after 72-h treatment with cisplatin, SB265610, or their concomitant combination at the indicated doses in DU145 cells; *p* values were relative to cisplatin alone. (D) Dot plot representing combination index values calculated for each combined treatment dose. (E) Representative colony assay images (left) and bar graph (right) representing the percentage (mean ± SEM) of colonies in DU145 cells after treatment with cisplatin, SB265610, or their combination at the indicated doses; *p* value was relative to cisplatin alone. (F) Representative colony assay images (left) and bar graph (right) representing the percentage (mean ± SEM) of colonies in DU145 cells after treatment with cisplatin, venetoclax, or their combination at the indicated doses; *p* value was relative to cisplatin alone. (G) Representative colony assay images (left) and bar graph (right) representing the percentage (mean ± SEM) of colonies in PC3 cells after treatment with cisplatin, venetoclax, or their combination at the indicated doses; *p* value was relative to cisplatin alone. (H) Dose-response curves for PC3-DR cells, after *CXCR2* overexpression (CXCR2ov), treated with 0–50 μM cisplatin for 72 h (mean ± SEM). (I) Representative colony assay images (left) and bar graph (right) representing the percentage (mean ± SEM) of colonies in PC3-DR cells, after CXCR2ov, treated with cisplatin at 0.25 μM for 24 h; *p* value was relative to empty control (Ctrl) treated with cisplatin. (J) Bar graph representing the percentage (mean ± SEM) of late apoptotic cells after 72 h of treatment with 10 μM cisplatin in PC3-DR cells after CXCR2ov; *p* value

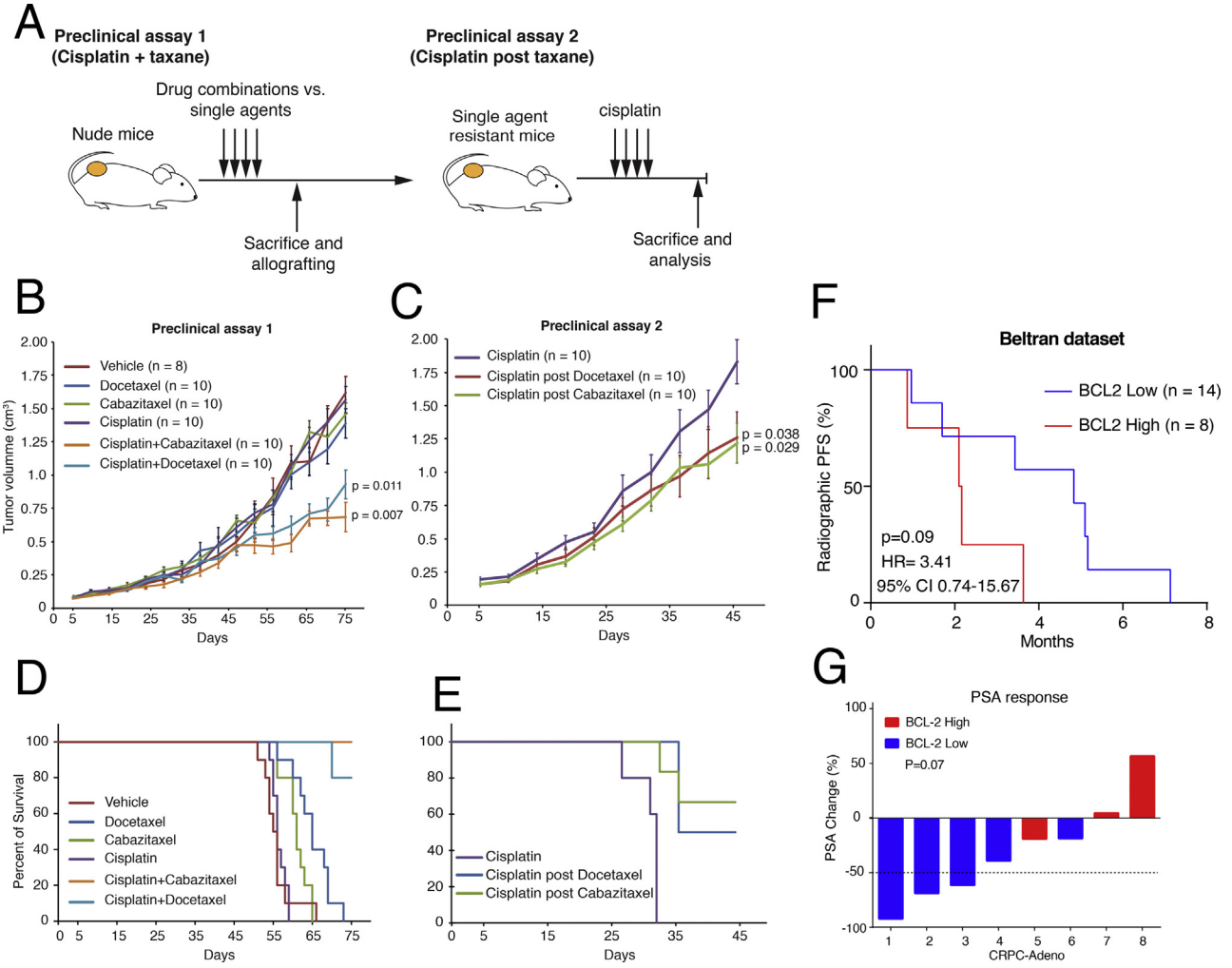

Fig. 5 – Preclinical validation. (A) Scheme of the preclinical assays carried out. Preclinical assay 1 assessed the antitumor efficacy of the single agent docetaxel, cabazitaxel, or cisplatin versus docetaxel plus cisplatin or cabazitaxel plus cisplatin. Single agent–treated tumors from preclinical assay 1 were shifted to cisplatin to test whether previous taxane exposure would sensitize for cisplatin treatment. (B) Tumor growth curves for NPK allografts treated with the indicated drugs or vehicle for 75 d. ANOVA is used to assess the significance of the differences in tumor growth; *p* values were relative to vehicle condition. (C) Tumor growth curves for single agent docetaxel- or cabazitaxel-treated, or vehicle-treated tumors from (B) under cisplatin treatment for 45 d. ANOVA is used to assess the significance of the differences in tumor growth; *p* values were relative to pretreated tumors with vehicle in (B). Kaplan-Meier survival curves for mice enrolled in (D) preclinical assay 1 or (E) preclinical assay 2. (F) Kaplan-Meier analysis for radiographic progression-free survival on platinum-based chemotherapy-treated patients in the Beltran dataset according to their BCL-2 expression by RNAseq (*n* = 21). Curves where compared using the log-rank test, with *p* value considered significant when <0.05. (G) Waterfall plot (*n* = 8) showing the magnitude of PSA decline in the subset of mCRPC adenocarcinomas within the cohort according to their BCL-2 expression. Fisher exact test with a significance level of 5% was used to measure the association between Bcl2 expression and PSA decline. ANOVA = analysis of variance; CI = confidence interval; CRPC = castration-resistant prostate cancer; HR = hazard ratio; mCRPC = metastatic castration-resistant prostate cancer; PFS = progression-free survival; PSA = prostate-specific antigen.

4. Discussion

Taxane-platinum combinations have shown clinical benefit for a subgroup of mCRPC patients [6], highlighting the need for predictive response indicators. Exploiting publicly available datasets, we have found that in taxane-exposed PC tumors, apoptosis and inflammatory response pathways are dysregulated and that the CXCR2/BCL-2 axis is reduced markedly. In vitro and in vivo assays showed that the loss of CXCR2 and BCL-2 represents an emerging vulnerability to genotoxic platinum-based treatments. Accordingly, interrogation of a cohort of platinum-treated mCRPC patients

was relative to empty Ctrl cells treated with cisplatin. (K) Dose-response curves for DU145-DR (top) and PC3-DR (bottom) cells, after *BCL-2* overexpression (BCL2ov), treated with 0–50 μM cisplatin for 72 h (mean ± SEM). (L) Representative colony assay images after treatment with cisplatin at 0.25 μM for 24 h in DU145-DR and PC3-DR cells, after BCL-2ov. (M) Bar graphs representing the percentage (mean ± SEM) of colonies after 24 h of treatment with cisplatin after BCL-2ov; *p* values were relative to BCL-2ov cells treated with cisplatin. (N) Western blot analysis of cleaved PARP protein expression changes after cisplatin treatment at the indicated doses in DU145-DR cells under empty Ctrl and *BCL-2* overexpression. β-actin was used as endogenous control. (O) Bar graph illustrating relative protein expression levels of cleaved PARP after cisplatin treatment at the indicated doses in DU145-DR cells. All results were obtained from at least three independent biological replicates. The *p* values were calculated using nonlineal regression and *F* test for viability, or two-tailed Student *t* test for clonogenic and apoptosis, and considered significant when <0.05. IC50 = half maximal inhibitory concentration; PC = prostate cancer; SEM = standard error of the mean; siControl = cells transfected with a silencer negative transcription control.

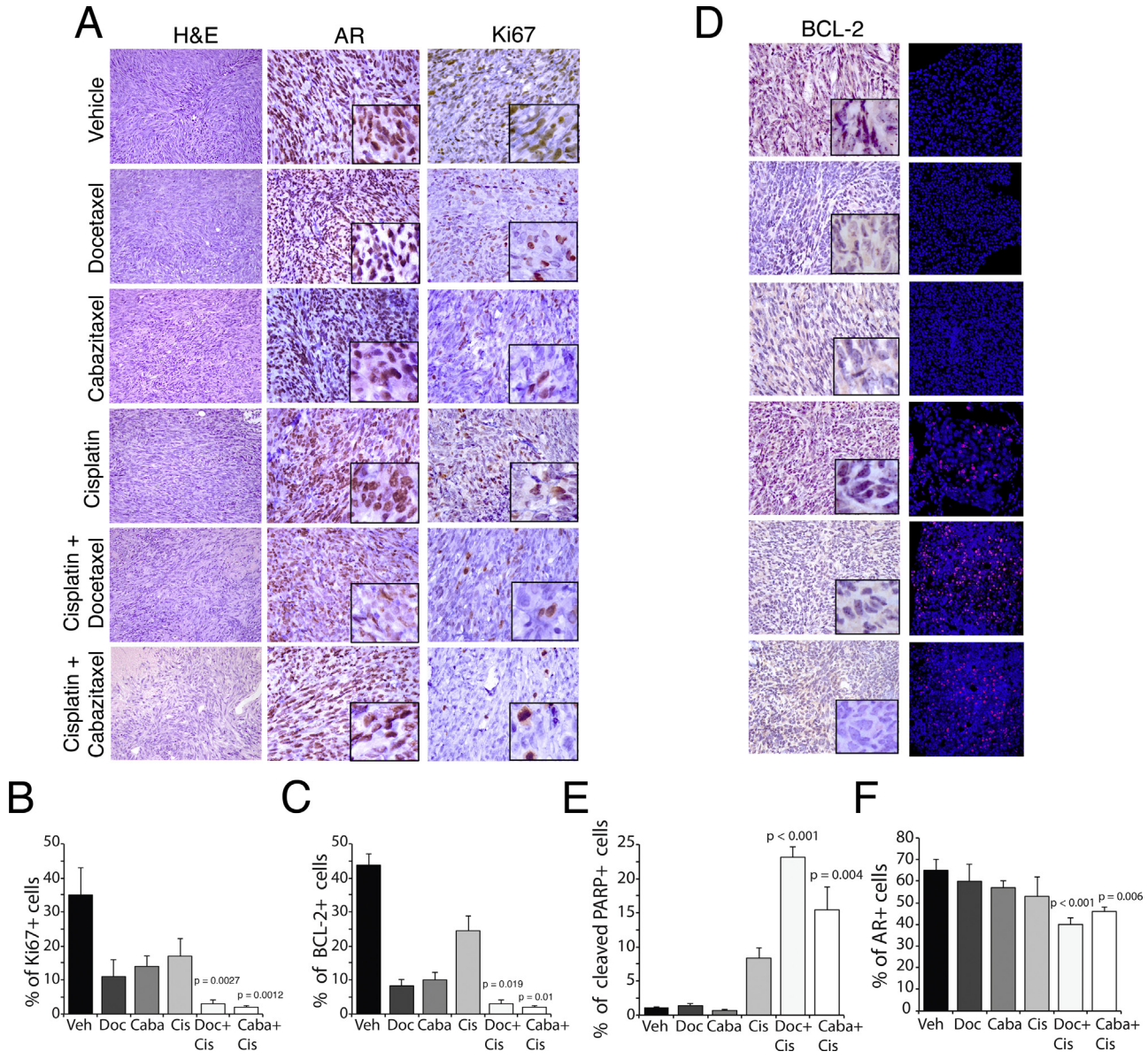

Fig. 6 – Histopathological analysis of preclinical cohorts. (A) Hematoxylin-eosin staining with immunohistochemistry for AR and Ki-67 in tumors from preclinical assay 1. Microphotogaphs are shown at 400× magnification and representative of five different mouse tumors. Insets correspond to 63× magnification. Quantification of (B) Ki-67 and (C) BCL-2. (D) Representative immunohistochemistry and immunofluorescence microphotographs for BCL-2 and cleaved PARP. Quantification of (E) cleaved PARP staining and (F) nuclear AR. Shown is the percent of positive nuclear stain over total number of cells in five different 40× magnifications fields from at least three independent mouse tumors; *p* values were relative to docetaxel or cabazitaxel treatment alone. The *p* values were calculated using two-tailed Student *t* test and considered significant when <0.05. AR = androgen receptor; Caba = cabazitaxel; Cis = cisplatin; Doc = docetaxel; H&E = hematoxylin and eosin; Veh = vehicle.

suggests an association with improved clinical response. Finally, in agreement with other studies [26], our preclinical trials in vivo confirm that taxane exposure sensitizes PC cells to platinum.

In addition to stabilizing microtubules, taxanes induce apoptosis by inhibiting antiapoptotic proteins, such as BCL-2 [27]. Accordingly, following treatment with paclitaxel, BCL-2 is phosphorylated in PC3 and LNCaP cells, inhibiting its antiapoptotic action and enhancing cell death [28,29]. Consistent with our results, BCL-2 downregulation after docetaxel treatment has been shown in breast cancer cells [30]. Downregulation of a drug's target and signaling rewiring to elicit prosurvival pathways is a well-known mechanism of cancer treatment resistance [31]. Therefore, our data suggest that mCRPC patients lose BCL-2 expression, at least in part, through CXCR2 downregulation as a mechanism to evade docetaxel-induced apoptosis. In agreement with previous data [16,22,23], we demonstrated that inhibition of the CXCR2 chemokine receptor markedly increased the sensitivity of AR-dependent and AR-independent PC cells to cisplatin treatment, suggesting that the inverse relationship between docetaxel resistance and cisplatin resistance could be mediated, at least in part, by CXCR2 downregulation after taxane exposure. Conversely, other studies also demonstrated

that when cells become resistant to platinum, they often become sensitive to taxanes [32,33].

In line with the findings from a recent phase I/II trial [24], our in vivo preclinical results in an AR-indifferent PC model suggest that therapeutic responses to cisplatin-based chemotherapy in docetaxel-resistant mCRPC patients might be predicted by CXCR2/BCL-2 expression. While we show that taxane consistently reduces CXCR2 and BCL2, only a subset of patients is expected to respond to taxane-platinum combinations, likely reflecting the inherent limitation of preclinical models in recapitulating the spectrum of heterogeneity. Finally, clinical qualification of CXCR2 and/or BCL-2 as a predictive biomarker will first require determining the most suitable analytical test and biospecimen. Our data using transcriptomics from the SU2C cohort to define expression thresholds subsequently used in the retrospective Beltran dataset illustrate the feasibility of this general approach to estimate the subset of patients expected to benefit from platinum-based combinations. Ultimately, cutoff thresholds to classify patients as those having low or high BCL-2 or CXCR2 expression and their association to treatment response will need to be tested and validated in independent prospective trials.

5. Conclusions

The CXCR2/BCL-2 antiapoptotic axis is markedly reduced in taxane-exposed mCRPC tumors, representing an emerging vulnerability to genotoxic platinum-based treatments. Therefore, taxane-resistant tumors are sensitized to cisplatin treatment, and taxane-cisplatin combinations have antitumor efficacy in aggressive mCRPC. Our findings also suggest that CXCR2/BCL-2 expression levels might predict therapeutic response to cisplatin-based treatment in docetaxel-resistant mCRPC patients.

***Author contributions*:** Albert Font and Alvaro Aytes had full access to all the data in the study and take responsibility for the integrity of the data and the accuracy of the data analysis.

Study concept and design: Ruiz de Porras, Martinez-Balibrea, Mellado, Font, Aytes.
Acquisition of data: Ruiz de Porras, Wang, Palomero, Marin-Aguilera, Indacochea, Bystrup, Solé-Blanch, Jimenez, Bakht, Conteduca.
Analysis and interpretation of data: Ruiz de Porras, Palomero, Indacochea, Mellado, Beltran, Aytes, Font.
Drafting of the manuscript: Ruiz de Porras, Aytes.
Critical revision of the manuscript for important intellectual content: All authors.
Statistical analysis: Ruiz de Porras, Palomero, Indacochea, Aytes.
Obtaining funding: Font, Aytes.
Administrative, technical, or material support: Ruiz de Porras, Wang, Palomero, Marin-Aguilera, Bystrup, Solé-Blanch, Jimenez.
Supervision: Font, Aytes.
Other: None.

***Financial disclosures*:** Albert Font and Alvaro Aytes certify that all conflicts of interest, including specific financial interests and relationships and affiliations relevant to the subject matter or materials discussed in the manuscript (eg, employment/affiliation, grants or funding, consultancies, honoraria, stock ownership or options, expert testimony, royalties, or patents filed, received, or pending), are the following: None

***Funding/Support and role of the sponsor*:** This work was supported by funding from the "Badalona Foundation Against Cancer" grant (Albert Font) and from Instituto de Salut Carlos III (PI16/01070 andCP15/00090; Alvaro Aytes), the European Association of Urology Research Foundation (EAURF/407003/XH; Alvaro Aytes),Fundacion BBVA (Alvaro Aytes), Department of Defense Award (W81XWH-18-1-0193; Alvaro Aytes), the CERCA Program/Generalitat de Catalunya (Alvaro Aytes), and FEDER funds/European Regional Development Fund (ERDF)—a way to Build Europe (Alvaro Aytes).

***Acknowledgments*:** Vicenç Ruiz de Porras and Albert Font acknowledge the "Badalona Foundation against cancer". Alberto Indacochea acknowledges the Spanish Ministry (MEIC) to EMBL partnership, Severo Ochoa, and the CERCA program.

Appendix A. Supplementary data

Supplementary material related to this article can be found, in the online version, at https://doi.org/10.1016/j.eururo.2020.10.001.

References

[1] Attard G, Parker C, Eeles RA, et al. Prostate cancer. Lancet 2016;387:70–82.
[2] Sartor O, de Bono JS. Metastatic prostate cancer. N Engl J Med 2018;378:645–57.
[3] Nuhn P, De Bono JS, Fizazi K, et al. Update on systemic prostate cancer therapies: management of metastatic castration-resistant prostate cancer in the era of precision oncology. Eur Urol 2019;75:88–99.
[4] Beltran H, Tomlins S, Aparicio A, et al. Aggressive variants of castration-resistant prostate cancer. Clin Cancer Res 2014;20:2846–50.
[5] Labrecque MP, Coleman IM, Brown LG, et al. Molecular profiling stratifies diverse phenotypes of treatment-refractory metastatic castration-resistant prostate cancer. J Clin Invest 2019;129:4492–505.
[6] Aparicio AM, Harzstark AL, Corn PG, et al. Platinum-based chemotherapy for variant castrate-resistant prostate cancer. Clin Cancer Res 2013;19:3621–30.
[7] Fitzpatrick JM, de Wit R. Taxane mechanisms of action: potential implications for treatment sequencing in metastatic castration-resistant prostate cancer. Eur Urol 2014;65:1198–204.
[8] Darshan MS, Loftus MS, Thadani-Mulero M, et al. Taxane-induced blockade to nuclear accumulation of the androgen receptor predicts clinical responses in metastatic prostate cancer. Cancer Res 2011;71:6019–29.
[9] Zhu ML, Horbinski CM, Garzotto M, Qian DZ, Beer TM, Kyprianou N. Tubulin-targeting chemotherapy impairs androgen receptor activity in prostate cancer. Cancer Res 2010;70:7992–8002.
[10] Lohiya V, Aragon-Ching JB, Sonpavde G. Role of chemotherapy and mechanisms of resistance to chemotherapy in metastatic castration-resistant prostate cancer. Clin Med Insights Oncol 2016;10:57–66.
[11] Antonarakis ES, Armstrong AJ. Evolving standards in the treatment of docetaxel-refractory castration-resistant prostate cancer. Prostate Cancer Prostatic Dis 2011;14:192–205.

[12] Hager S, Ackermann CJ, Joerger M, Gillessen S, Omlin A. Anti-tumour activity of platinum compounds in advanced prostate cancer-a systematic literature review. Ann Oncol 2016;27:975–84.
[13] Abida W, Cyrta J, Heller G, et al. Genomic correlates of clinical outcome in advanced prostate cancer. Proc Natl Acad Sci USA 2019;116:11428–36.
[14] Gao J, Aksoy BA, Dogrusoz U, et al. Integrative analysis of complex cancer genomics and clinical profiles using the cBioPortal. Sci Signal 2013;6:pl1.
[15] Marin-Aguilera M, Codony-Servat J, Kalko SG, et al. Identification of docetaxel resistance genes in castration-resistant prostate cancer. Mol Cancer Ther 2012;11:329–39.
[16] Ruiz de Porras V, Bystrup S, Martinez-Cardus A, et al. Curcumin mediates oxaliplatin-acquired resistance reversion in colorectal cancer cell lines through modulation of CXC-Chemokine/NF-kappaB signalling pathway. Sci Rep 2016;6:24675.
[17] Aytes A, Mitrofanova A, Kinkade CW, et al. ETV4 promotes metastasis in response to activation of PI3-kinase and Ras signaling in a mouse model of advanced prostate cancer. Proc Natl Acad Sci USA 2013;110:E3506–15.
[18] Aytes A, Giacobbe A, Mitrofanova A, et al. NSD2 is a conserved driver of metastatic prostate cancer progression. Nat Commun 2018;9: 5201.
[19] Maxwell PJ, Coulter J, Walker SM, et al. Potentiation of inflammatory CXCL8 signalling sustains cell survival in PTEN-deficient prostate carcinoma. Eur Urol 2013;64:177–88.
[20] Richardson RM, Pridgen BC, Haribabu B, Ali H, Snyderman R. Differential cross-regulation of the human chemokine receptors CXCR1 and CXCR2. Evidence for time-dependent signal generation. J Biol Chem 1998;273:23830–6.
[21] Singh RK, Lokeshwar BL. Depletion of intrinsic expression of Interleukin-8 in prostate cancer cells causes cell cycle arrest, spontaneous apoptosis and increases the efficacy of chemotherapeutic drugs. Mol Cancer 2009;8:57.
[22] Wilson C, Purcell C, Seaton A, et al. Chemotherapy-induced CXC-chemokine/CXC-chemokine receptor signaling in metastatic prostate cancer cells confers resistance to oxaliplatin through potentiation of nuclear factor-kappaB transcription and evasion of apoptosis. J Pharmacol Exp Ther 2008;327:746–59.
[23] Ning Y, Labonte MJ, Zhang W, et al. The CXCR2 antagonist, SCH-527123, shows antitumor activity and sensitizes cells to oxaliplatin in preclinical colon cancer models. Mol Cancer Ther 2012;11: 1353–64.
[24] Corn PG, Heath EI, Zurita A, et al. Cabazitaxel plus carboplatin for the treatment of men with metastatic castration-resistant prostate cancers: a randomised, open-label, phase 1-2 trial. Lancet Oncol 2019;20:1432–43.
[25] Conteduca V, Ku SY, Puca L, et al. SLFN11 Expression in advanced prostate cancer and response to platinum-based chemotherapy. Mol Cancer Ther 2020;19:1157–64.
[26] Locke VL, Davey RA, Davey MW. Modulation of drug and radiation resistance in small cell lung cancer cells by paclitaxel. Anticancer Drugs 2003;14:523–31.
[27] Haldar S, Basu A, Croce CM. Bcl2 is the guardian of microtubule integrity. Cancer Res 1997;57:229–33.
[28] Haldar S, Chintapalli J, Croce CM. Taxol induces bcl-2 phosphorylation and death of prostate cancer cells. Cancer Res 1996;56: 1253–5.
[29] Miayake H, Tolcher A, Gleave ME. Chemosensitization and delayed androgen-independent recurrence of prostate cancer with the use of antisense Bcl-2 oligodeoxynucleotides. J Natl Cancer Inst 2000;92:34–41.
[30] Dey G, Bharti R, Das AK, Sen R, Mandal M. Resensitization of Akt induced docetaxel resistance in breast cancer by 'Iturin A' a lipopeptide molecule from marine bacteria *Bacillus megaterium*. Sci Rep 2017;7:17324.
[31] Vasan N, Baselga J, Hyman DM. A view on drug resistance in cancer. Nature 2019;575:299–309.
[32] Stordal BK, Davey MW, Davey RA. Oxaliplatin induces drug resistance more rapidly than cisplatin in H69 small cell lung cancer cells. Cancer Chemother Pharmacol 2006;58:256–65.
[33] Stordal B, Pavlakis N, Davey R. A systematic review of platinum and taxane resistance from bench to clinic: an inverse relationship. Cancer Treat Rev 2007;33:688–703.